

Flammability and thermal behaviors of polypropylene composite containing modified kaolinite

Wufei Tang, Xiaoyu Gu, Yu Jiang, Jingran Zhao, Wenjun Ma, Peng Jiang, Sheng Zhang

Key Laboratory of Carbon Fiber and Functional Polymers (Ministry of Education, Beijing University of Chemical Technology), Beijing 100029, China

Correspondence to: X. Gu (E-mail: guxy@mail.buct.edu.cn)

ABSTRACT: Exfoliated kaolinite (E-Kaol) was prepared by intercalating DMSO and KAc into kaolinite successively followed by irradiation under ultrasonic. The modified kaolinite was then introduced to polypropylene (PP) by melt blending in order to improve the fire performance of the composite. The flammability and thermal behaviors of PP composite were analyzed by limit oxygen index, vertical burning test, cone calorimeter test, and thermal-gravimetric analysis, respectively. The microstructure of PP composites was characterized by Fourier-transformed infrared spectroscopy, X-ray diffraction, and scanning electron microscope (SEM). It was demonstrated the presence of only 1 phr E-Kaol could improve the LOI values of PP/microencapsulated ammonium polyphosphate (MCAPP)/ATH composite from 26.4 to 28.0, and decrease the peak value of heat release rate and smoke production rate of the PP/MCAPP/ATH by 60.7% and 39.1%, respectively, compared with that of PP sample. Morphology analysis by SEM showed that E-Kaol in PP composite was beneficial to forming rigid and compact char structure. © 2014 Wiley Periodicals, Inc. *J. Appl. Polym. Sci.* **2015**, *132*, 41761.

KEYWORDS: clay; composites; degradation; flame retardance; thermoplastics

Received 22 July 2014; accepted 12 November 2014

DOI: 10.1002/app.41761

INTRODUCTION

Nowadays, polypropylene (PP) has been widely used in daily life, medical and defense sectors, and other fields due to its light weight, chemical corrosion resistance, and excellent mechanical properties and so on. However, its inherent inflammability and high amount heat release during combustion have restricted its application. Therefore, PP is required to be modified to meet safety standards^{1–4} in many cases. Non-halogenated flame retardant, such as intumescent system, metal hydroxides, and natural clays have been popularly utilized in PP.^{5–9}

Among the metallic hydroxide flame retardants, aluminumhydroxide (ATH) is a kind of popular flame retardant by releasing water vapor and endothermic decomposition leaving a thermally stable inorganic residue.¹⁰ However, high ATH loading (more than 60%) is usually required in order to obtain good flame retardant performance. As a result ATH has been usually used conjunctively with other flame retardants to reduce the negative effect on mechanical properties of the material.

Ammonium polyphosphate (APP) has attracted much attention for its excellent performance, such as safe environmental protection, high phosphorus and nitrogen content, and good thermal stability.^{11–13} On the other hand, APP is difficult to satisfy the standards in damp environment because of its poor compatibil-

ity with polymer matrix and relative high water absorption. Surface modification such as microcapsules or surfactant processing^{14–16} is often used to improve the compatibility of APP with polymer matrix.

Since the 1990s, layered silicates nanocomposites (PLS) including layered double hydroxides (LDH) and montmorillonite (MMT) have been introduced to polymers to reduce the flame spreading rate. It has been proved that the introduction of layered silicates to polymers can improve mechanical properties, thermal stability, fire-resistance, and smoke suppression^{17–20} of the substrate.

Kaolinite is alumino-silicate clays ($\text{Al}_2[(\text{OH})_4/\text{Si}_2\text{O}_5]$) mined from natural deposits. It is chemically similar to halloysite nanotubes, but differs by having a predominantly plate-like structure, rather than hollow microtubular structure. Unlike MMT, kaolinite belongs to the non-expensive layered silicates; there are no exchangeable ions in the gallery space. In kaolinite, the layers are built of only one sheet of silicon that is covered by oxygen atoms and one sheet of aluminum that is covered by hydroxyl groups.²¹ Kaolinite is more difficult to be intercalated and exfoliated compared with MMT and LDH. Layer structure-induced asymmetric effects of kaolinite and hydrogen bonding between the layers lead to high inter-layer adhesion, as a result only small and high polar

Table I. Formulation, LOI, and UL-94 Tests of PP Composites

Sample	PP	MCAPP	ATH	Kaolinite	E-Kaol	LOI (%) (± 0.2)	Time to dripping (s) (± 2)	UL-94 rating
PP	100	-	-	-	-	18.0	4	NR
PP/MCAPP/ATH	75	16.7	8.3	-	-	26.4	36	NR
PP/MCAPP/ATH/kaolinite	75	16.7	8.3	1	-	27.0	46	NR
	75	16.7	8.3	3	-	25.2	50	NR
	75	16.7	8.3	5	-	24.7	51	NR
	75	16.7	8.3	10	-	23.6	54	NR
PP/MCAPP/ATH/E-Kaol	75	16.7	8.3	-	1	28.0	49	NR
	75	16.7	8.3	-	3	25.6	53	NR
	75	16.7	8.3	-	5	24.9	55	NR
	75	16.7	8.3	-	10	24.0	58	NR

molecules, such as hydrazine and DMSO, can intercalate into the interlayers of kaolinite directly.^{22,23} The intercalation and exfoliation structure can significantly improve the dispersion of kaolinite in polymer substrate, and is beneficial to enhancing mechanical properties and fire resistance of polymer/kaolinite composite. Although some efforts have been made on improving the flame retardancy by incorporating kaolinite into polymers,²⁴ the effects of modified kaolinite on the fire performance and thermal behavior of PP have not been reported so far.

This study reports the preparation of exfoliated kaolinite (E-Kaol) by intercalating DMSO and KAc successively followed by ultrasonic irradiation. APP was coated with melamine (MA) to prepare microencapsulated ammonium polyphosphate (MCAPP). The E-Kaol in association with MCAPP/ATH was used to improve the flame retardancy of PP. The thermal stability was investigated by thermal-gravimetric analysis (TGA). The fire performance of PP composite was characterized by limit oxygen index (LOI), vertical burning test (UL-94) and cone calorimeter test (CONE). The morphology of char residue was examined by scanning electron microscope (SEM) and Fourier-transformed infrared spectroscopy (FTIR).

EXPERIMENTAL

Materials

A commercial PP with a melt flow index of 3 g/10 min was provided by Sinopec Maoming Company (Maoming, China). APP was purchased from Jin Ying Tai Chemical Co. (Jinan, China). MA was obtained from Jin Tong Le Tai Chemical Product Co. (Beijing, China). Formaldehyde (POM), aluminum hydroxide (ATH), dimethyl sulfoxide (DMSO), and potassium acetate (KAc) were supplied by Beijing Chemical Factory (Beijing, China). The raw kaolinite was provided from Xing Yi Mineral Processing Plant (Shijiazhuang, China).

Preparation of Exfoliated Kaolinite

About 4 g kaolinite was firstly dispersed in a mixture of 40 mL DMSO and 4.5 mL deionized water. The suspension was reacted under ultrasonic with a power of 800 W for 4 h. After reaction the solid product was filtered three times with ethanol to clear away residuary DMSO, and then dried at 60°C for about 12 h (D-Kaol). The D-Kaol sample (2 g) was then mixed with 40 mL saturated KAc water solution under magnetic stirring at 50°C for 24 h. The reacted mixture was washed with ethanol three times, and then filtrated before dried at 60°C for 12 h (KAc-Kaol). Finally, the KAc-Kaol sample (0.4 g) and 30 mL water

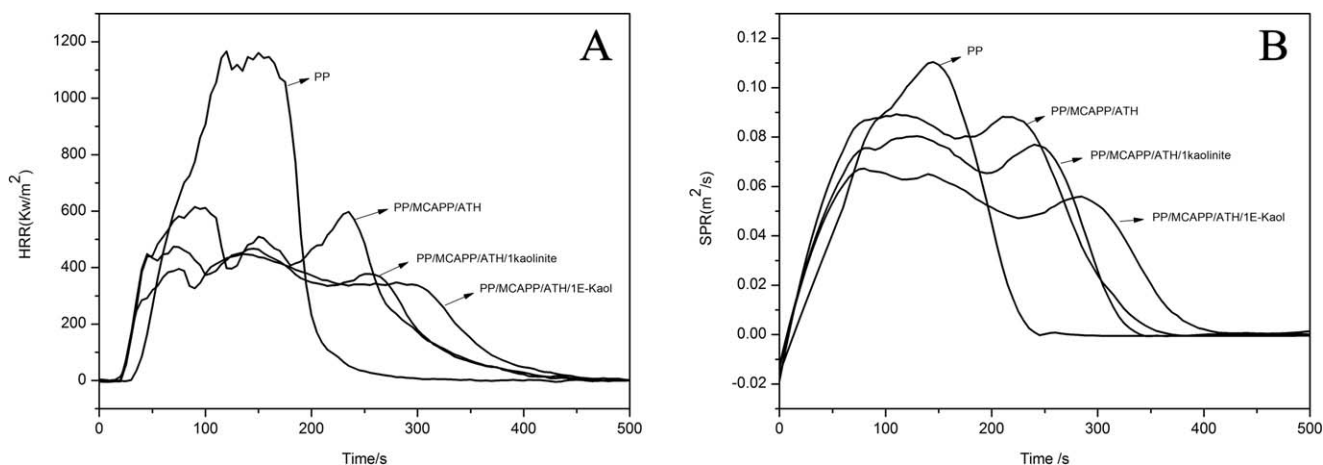


Figure 1. Cone results of PP and its composites. A: HRR curves, (B) SPR curves.

Table II. Key Cone Calorimeter Data of PP Composite

Samples	PHRR (kW/m ²)	TTI (s)	T _{PHRR} (s)	FPI (m ² s/kW)	FGI (kW/m ² s)	AMLR (g/s)	AHRR (kW/m ²)
PP	1166 ± 23	27 ± 2	120 ± 2	0.023	9.72	0.138 ± 0.004	744 ± 12
PP/MCAPP/ATH	615 ± 19	18 ± 1	89 ± 2	0.029	6.91	0.089 ± 0.003	457 ± 10
PP/MCAPP/ATH/1kaolinite	474 ± 17	17 ± 1	71 ± 1	0.036	6.68	0.080 ± 0.003	397 ± 9
PP/MCAPP/ATH/1E-Kaol	448 ± 14	19 ± 1	134 ± 2	0.042	3.34	0.073 ± 0.002	369 ± 7

was mixed under ultrasonic (1000 W) for 1 h. The product was purified with ethanol three times before being filtrated and dried at 60°C for 12 h. The E-Kaol was then obtained.

Preparation of Composites

The composites were prepared by melt blending with a micro twin-screw extruder (Wuhan Rui Ming Plastics Machinery Co.). The processing temperatures of different sections were maintained at 160, 180, and 200°C, respectively.

Table I presents the formulation of PP composites.

Characterization

The X-ray diffraction (XRD) was performed with D/max-2500 diffraction. The CuK α radiation source was operated at 40 kV and 20 mA ($\lambda = 0.154$ nm). Samples were scanned from 3 to 30° at a scan rate of 2°/min. The interlayer space of clay was calculated according to Bragg's equation:

$$\lambda = 2d\sin\theta \quad (1)$$

where d is the basal spacing, θ is the diffraction angle.

TGA analysis was conducted using a synchronous thermal analyzer (STA449C, Netzsch) from 30 to 800°C at a heating rate of 10°C/min.

LOI and UL-94 vertical burning test was tested according to the standard oxygen index test method of ISO 4589-2. The results presented were an average of five replicates.

Evaluation of flammability of the composites was performed using cone calorimeter (FFT Co.) according to the ISO 5660

standard. The samples with a dimension of 100 × 100 × 3 mm³ were tested at horizontal position with heat radiant flux density of 50 kW/m². Specimens were wrapped in aluminum foil, leaving the upper surface exposed to the radiator. The experiments were repeated five times. Relative parameters such as heat release rate (HRR), time to ignition (TTI), mass loss rate (MLR), and smoke production rate (SPR) were obtained and summarized.

The morphological features of composites and the char residues after combustion in cone calorimeter were observed by a Hitachi S-4700 SEM under the voltage of 20 kV.

The char residues after combustion in cone calorimeter were also characterized by FTIR (Nicolet IS5 under the resolution of 1 cm⁻¹ in 32 scans) using KBr pellets.

RESULTS AND DISCUSSION

Flammability

LOI and UL-94 Tests. Table I presents the LOI values and UL-94 ratings of neat PP and its composites. The LOI value of neat PP was only 18, however, the LOI of PP composite containing MCAPP and ATH was increased to 26.4. The introduction of 1 phr kaolinite or E-Kaol could further increase the LOI value to 27.0 and 28.0, respectively. However, further addition of kaolinite or E-Kaol could decrease the LOI values. It was proposed that kaolinite could be well dispersed in PP matrix at low concentration, which could improve the distribution of flame retardants whose functional groups were attracted inside

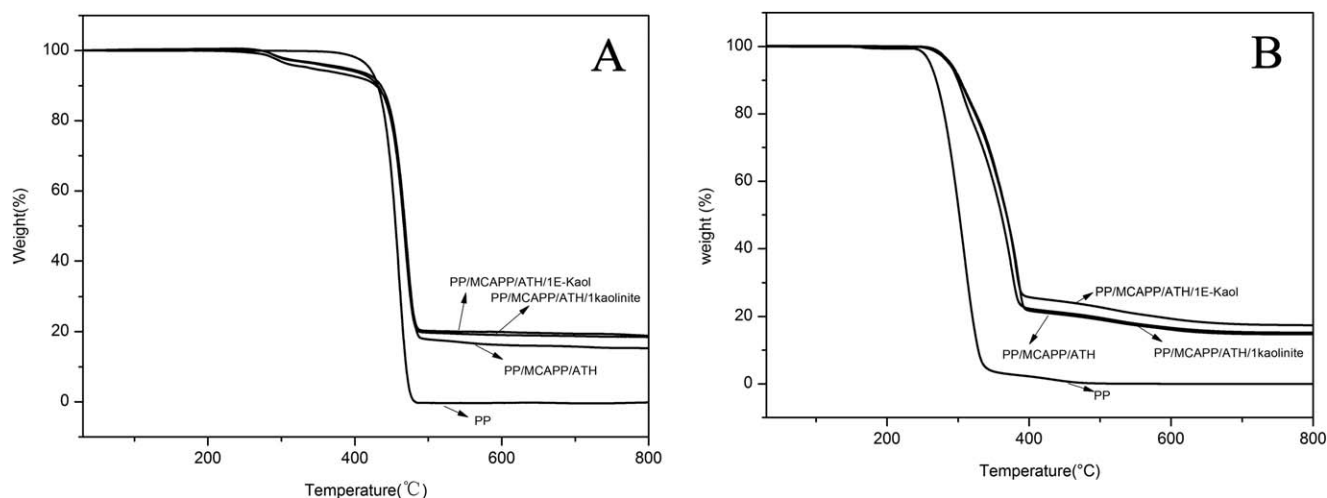


Figure 2. TGA curves of PP and its composites. A: Nitrogen atmosphere, (B) air atmosphere.

Table III. Key Data of TGA Curves of PP Composites

Samples	N ₂ atmosphere			Air atmosphere		
	T _{0.05} (°C)	T _{0.5} (°C)	Residues (wt %)	T _{0.05} (°C)	T _{0.5} (°C)	Residues (wt %)
PP	420	455	0	261	302	0
PP/MCAPP/ATH	339	468	16.2	289	368	14.8
PP/MCAPP/ATH/1kaolinite	378	467	19.0	288	360	15.3
PP/MCAPP/ATH/1E-Kaol	388	468	20.1	287	368	17.7

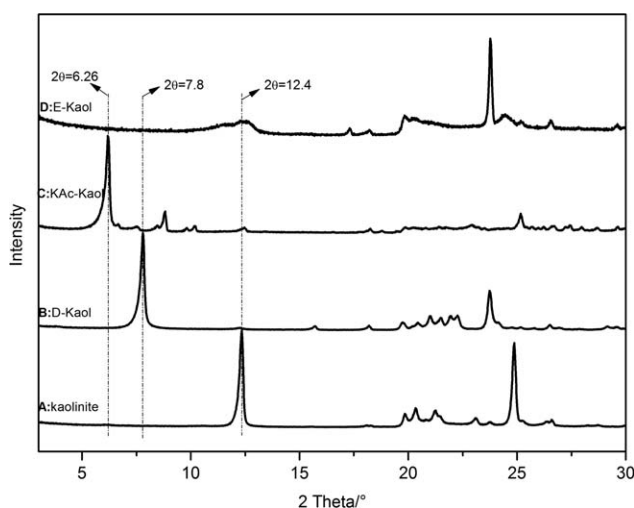
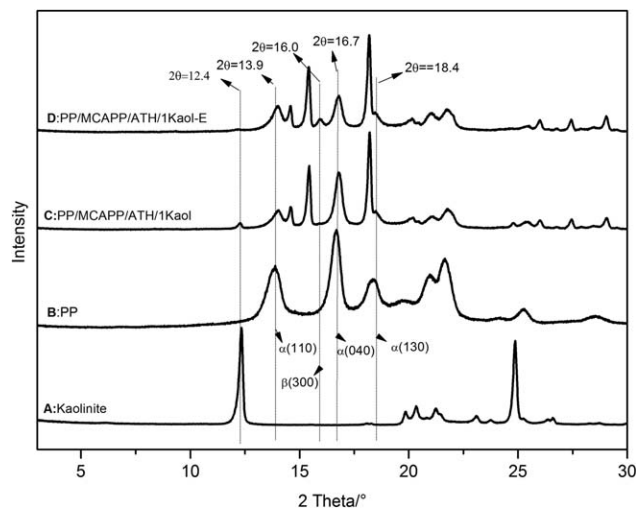
kaolinite layers. It was proposed that kaolinite could catalyze the degradation of PP composite, which results in the decrease of LOI.²⁵ The neat PP and its composites failed in UL-94 tests, however, the time to dropping (the time to the appearance of first molten drop, TD) in UL-94 tests was significantly prolonged after the introduction of kaolinite or E-Kaol. The TD for neat PP was 4 s, but it was increased to 36 s for PP/MCAPP/ATH. The incorporation of 1, 3, 5, 10 phr kaolinite prolonged TD to 46, 50, 51, and 54 s respectively, and the addition of E-Kaol further increased the TD to 49, 53, 55, and 58 s. The results indicated that E-Kaol was more effective than Kaolinite on hindering the spread of fire in PP.

Cone Calorimetry. Cone calorimeter can well describe a large scale fire test and be used to predict the combustion behavior of materials in a real fire.^{26,27} Figure 1 shows the HRR and SPR curves of PP composites, respectively. Some key data is summarized in Table II.

The neat PP burned very quickly after ignition and had a very strong peak heat release rate (PHRR) of 1166 kW/m² [Figure 1(A)]. Even though the addition of MCAPP/ATH could reduce the ignition time and prolonged the whole combustion process, it could significantly reduce the PHRR to 615 kW/m² which was 47.3% less than that of the neat PP. After the addition of 1 phr kaolinite or E-Kaol into PP/MCAPP/ATH, the PHRR was further reduced to 474 or 448 kW/m², respectively.

Smoke suppression is also important to evaluate the flame retardancy. It can be seen from Figure 1(B) that the peak of SPR of neat PP was 0.11 m²/s, and it was significantly decreased to 0.089 m²/s after adding MCAPP/ATH, and further decreased after introduction of kaolinite (0.08 m²/s) or E-Kaol (0.067 m²/s). At same time the smoke release process obviously prolonged, especially after the incorporation of E-Kaol.

Fire performance index (FPI) (TTI/PHRR) and fire growth index (FGI) (PHRR/T_{PHRR}) are very important parameters in evaluating the fire performance of polymer. Table II gives key cone calorimeter data of PP composite. One could see that FPI was increased from 0.023 m² s/kW of neat PP to 0.029 m² s/kW of PP containing MCAPP/ATH, and further increased to 0.036 and 0.042 m² s/kW after adding 1 phr kaolinite or E-Kaol, respectively. FGI value, which reflected the spread rate of fire, was significantly decreased from 9.72 kW/m² s in neat PP to 6.91 kW/m² s in PP/MCAPP/ATH, and was further dropped to 6.68 kW/m² s and 3.34 kW/m² s after the addition of 1 phr kaolinite and 1 phr E-Kaol, respectively. It is suggested both kaolinite and E-Kaol exhibit positive effects on improving the flame retardancy of PP, and E-Kaol is more effective than kaolinite. It is proposed that the more uniformly distribution of E-Kaol in PP matrix is beneficial to forming more compact char layer during combustion which could act as a barrier to isolate flame, heat, oxygen, and other volatile gases.

**Figure 3.** XRD patterns of different kaolinites.**Figure 4.** XRD patterns of kaolinite, PP, and its composites.

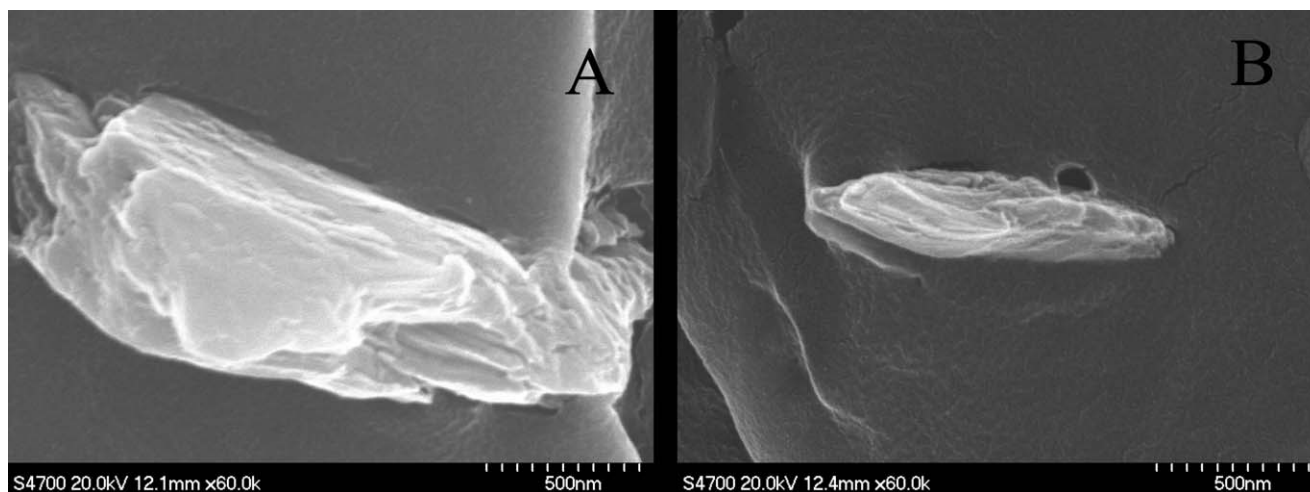


Figure 5. SEM images of PP composites. A: PP/MCAPP/ATH/1kaolinite, (B) PP/MCAPP/ATH/1E-Kaol.

Thermal Stability

The TGA curves of PP and its composites are shown in Figure 2. The temperature corresponding to 5 and 50 wt % weight loss ($T_{0.05}$ and $T_{0.5}$) are summarized in Table III.

Figure 2(A) shows the TGA curves of the PP and its composites under nitrogen atmosphere. Only a one-step decomposition was observed in neat PP during 400–500°C. Thermal decomposition of PP/MCAPP/ATH sample included two steps: the initial decomposition temperature ($T_{0.05}$) was 339°C, which was lower than that of PP (420°C) due to early decomposition of MCAPP/ATH; the second step of mass loss was the main decomposition process of polymer. The introduction of 1 phr kaolinite or E-Kaol increased the $T_{0.05}$ of PP/MCAPP/ATH significantly (from 339 to 378 and 388°C, respectively). The char residue at 700°C for neat PP was almost zero, whereas the remained char after adding flame retardants was about 16.2%, furthermore the char amount increased to 19.0% or 20.1% after addition of only 1 phr kaolinite or E-Kaol, which demonstrated that the presence of kaolinite could promote the char formation of PP composite. Figure 2(B) shows the TGA curves of the PP and its composites under air atmosphere. Interestingly, the curves showed different decomposition process compared to that under nitrogen atmosphere. During the process of oxidation degradation, oxidative dehydrogenation of the PP chain resulted from the hydrogen abstraction leads to the reduction of the thermal stability of PP.⁴ $T_{0.05}$ and $T_{0.5}$ of PP were 261 and

302°C, respectively, while $T_{0.05}$ of PP/MCAPP/ATH, PP/MCAPP/ATH/1kaolinite, and PP/MCAPP/ATH/1E-Kaol samples were increased to 289, 288, and 287°C, respectively. Only slight differences can be observed for $T_{0.5}$ of PP/MCAPP/ATH/1kaolinite, PP/MCAPP/ATH, and PP/MCAPP/ATH/1E-Kaol (in the range from 360 to 368°C). Char residue at 700°C of PP/MCAPP/ATH was 14.8%, it was increased to 15.3 and 17.7% after the introduction of 1 phr kaolinite and 1 phr E-Kaol, respectively.

It was suggested that good distribution of a low amount of flake clay in the matrix was conducive to form a barrier during heating²⁵ and the introduction of kaolinite or E-Kaol could enhance the thermal stability of the PP/MCAPP/ATH composite and improve the amount of char residue at high temperature.

Distribution of E-Kaol

The XRD patterns of kaolinite and E-Kaol are presented in Figure 3. The peak at 12.4° of kaolinite corresponds to 001 crystal phase with a basal spacing of 0.72 nm [Figure 3(A)]. The peak of 001 crystal phase for DMSO-Kaol decreased to 7.8° which corresponds to the basal spacing of 1.13 nm [Figure 3(B)].^{28,29} After further treatment with KAc, the diffraction degree of 001 left shifted further to 6.3° that meant the basal spacing of KAc-Kaol was increased to 1.41 nm.²¹ After irradiation of ultrasonic, the 001 peak almost disappeared [Figure 3(D)], which suggested that the lamellae in E-Kaol were almost exfoliated.

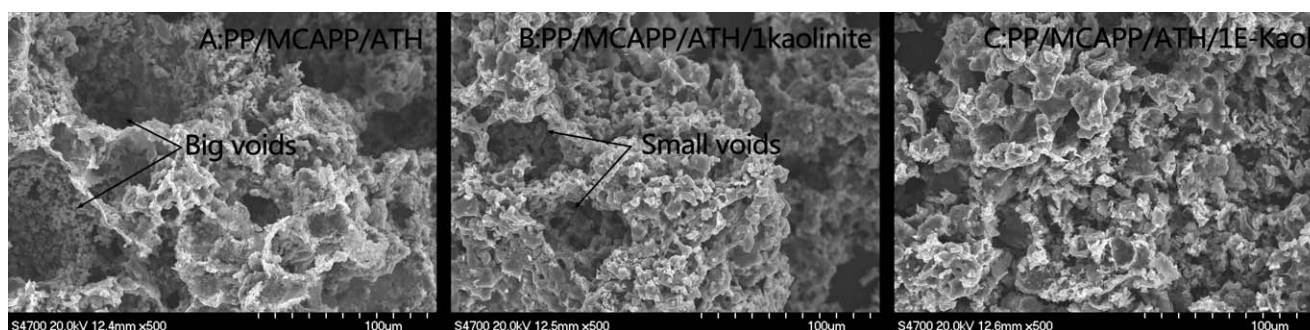


Figure 6. SEM images of the char of PP composites.

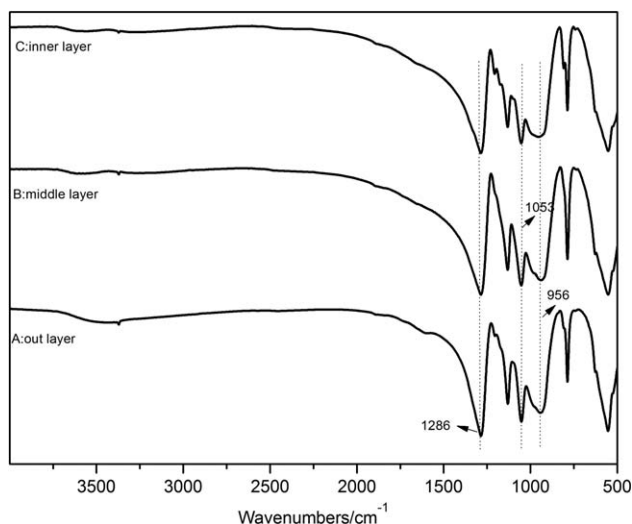


Figure 7. FTIR curves of the char of PP/MCAPP/ATH.

Figure 4 shows the XRD patterns of PP composites with 1 phr kaolinite or E-Kaol. Compared with neat PP, the position of characteristic peaks of α form at 13.9° (110), 16.7° (040), and 18.4° (130) varied little, but the relative peak intensity decreased obviously. The emergence of a new peak at 16.0° indicated the formation of β phase^{30–32} [Figure 4(D)]. It is concluded that a small amount of E-Kaol acts as heterogeneous additive which can induce the orientation of α phase and formation of β phase.

The 001 plane of kaolinite still existed in the composite containing kaolinite [Figure 4(C)], which indicated PP molecular chains could not intercalate easily into the crystal planes of raw kaolinite.

The microstructure of composites and the char was investigated by SEM. Figure 5 shows the SEM images of PP/MCAPP/ATH/1kaolinite and PP/MCAPP/ATH/1E-Kaol. It could be observed [Figure 5(A)] that the scattered size of kaolinite was obviously

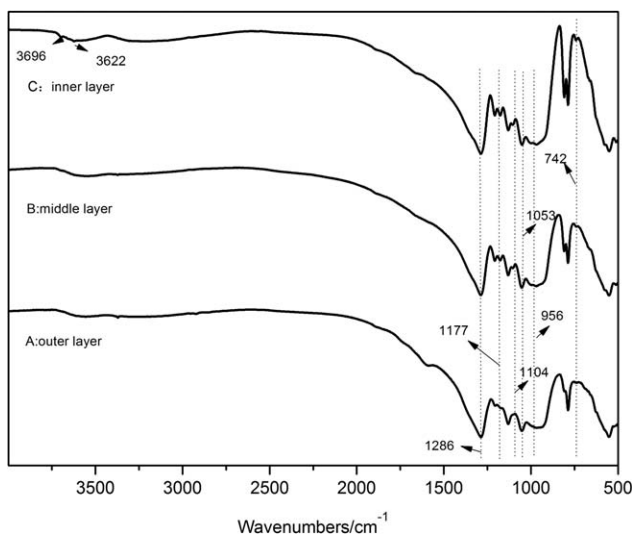


Figure 8. FTIR curves of the char of PP/MCAPP/ATH/1E-Kaol.

larger than that of E-Kaol, indicating the E-Kaol had better compatibility with PP than kaolinite.

Char

Figure 6 shows the SEM images of the char of PP composites. Uneven structure with big voids and cracks in PP/MCAPP/ATH could be observed from Figure 6(A). Voids in PP/MCAPP/ATH/1kaolinite were smaller than that in PP/MCAPP/ATH, which were shown in Figure 6(B). Almost no voids could be found from Figure 6(C) for the char surface of the sample containing 1 phr E-Kaol, indicating more compact and rigid char was formed.

During burning, MCAPP or ATH reacted with kaolinite to form ceramic-like aluminophosphate materials, which was favorable to form char with high quality.

Figures 7 and 8 show the FTIR spectra of different char layers of PP/MCAPP/ATH and PP/MCAPP/ATH/1 E-Kaol samples.

Figure 7 shows the relative intensity and position of some characteristic peaks at different depth of PP/MCAPP/ATH char sample, such as P=O at 1286 cm^{-1} , C—O at 1053 cm^{-1} , and C—C at 956 cm^{-1} ,^{33,34} is similar.

Figure 8 shows that the outer layer char in PP/MCAPP/ATH is very similar to that of PP/MCAPP/ATH/1E-Kaol. However, peaks at 1177 , 1104 , and 742 cm^{-1} corresponding to stretching absorption of C—N, P—O—C and C—H⁹ could be found both in the middle layer [Figure 8(B)] and interlayer [Figure 8(C)], respectively. The peaks at 3696 and 3622 cm^{-1} which were attributed to O—H of E-Kaol existed in the inner layer [Figure 8(C)].^{28,35,36}

The results indicated that most E-Kaol remained in the char after combustion, which was helpful to form a barrier. This structure could effectively restrict the oxygen and volatile gases diffusion during burning process.

CONCLUSIONS

E-Kaol was successfully prepared by a three-step method, and was introduced to PP/ATH/MCAPP to fabricate flame retardant composite. The introduction of small amount of kaolinite could significantly improve the flame retardancy of the PP composites, and E-Kaol showed a better performance in improving the fire-resistance of PP than raw kaolinite. Both kaolinite and E-Kaol could effectively improve the thermal degradation and formation of the char residues of PP composites. It was suggested that kaolinite was similar to analogous nanoclay which could improve the fire performance of the composite via forming a thermal insulation barrier during the burning.

ACKNOWLEDGMENTS

The authors would like to thank the National Natural Science Foundation of China (No.21374004 and No.51373018) for their financial support.

REFERENCES

- Zhang, S.; Horrocks, A. R. *Prog. Polym. Sci.* **2003**, *28*, 1517.
- Chen, X. L.; Jiao, C. M. *Fire. Saf. J.* **2009**, *44*, 1010.

3. Feng, C. M.; Zhang, Y.; Liu, S. W.; Chi, Z. G.; Xu, J. R. *Polym. Degrad. Stab.* **2012**, *97*, 707.
4. Du, M. L.; Guo, B. C.; Jia, D. M. *J. Eur. Polym.* **2006**, *42*, 1236.
5. Su, X. Q.; Yi, Y. W.; Tao, J.; Qi, H. Q. *Polym. Degrad. Stab.* **2012**, *97*, 2128.
6. Cao, K.; Wu, S. L.; Qiu, S. L.; Li, Y.; Yao, Z. *Ind. Eng. Chem. Res.* **2013**, *52*, 309.
7. Edward, D. W.; Sergei, V. L. *J. Fire. Saf.* **2008**, *26*, 5.
8. Marney, D. C. O.; Russell, L. J.; Wu, D. Y.; Nguyen, T.; Cramm, D.; Rigopoulos, N.; Wright, N.; Greaves, M. *Polym. Degrad. Stab.* **2008**, *93*, 1971.
9. Zhang, Y. D.; Xiang, J. J.; Zhang, Q.; Liu, Q. F.; Frost, F. L. *Thermochim. Acta* **2014**, *576*, 39.
10. Hollingbery, L. A.; Hull, T. R. *Polym. Degrad. Stab.* **2010**, *95*, 2213.
11. Yang, D. D.; Hu, Y.; Song, L.; Nie, S. B.; He, S. Q.; Cai, Y. B. *Polym. Degrad. Stab.* **2008**, *93*, 2014.
12. Jin, F. F.; Xia, Y.; Mao, Z. W.; Ding, Y. F.; Guan, Y.; Zheng, A. N. *Polym. Degrad. Stab.* **2014**, *110*, 252.
13. Dong, M. Z.; Gu, X. Y.; Zhang, S. *Ind. Eng. Chem. Res.* **2014**, *53*, 8062.
14. Shao, Z. B.; Deng, C.; Tan, Y.; Chen, M. J.; Chen, L.; Wang, Y. Z. *Polym. Degrad. Stab.* **2013**, *10*, 1.
15. Saihi, D.; Vroman, I.; Giraud, S.; Bourbigot, S. *React. Funct. Polym.* **2005**, *64*, 127.
16. Saihi, D.; Vroman, I.; Giraud, S.; Bourbigot, S. *React. Funct. Polym.* **2006**, *66*, 1118.
17. Huang, G. B.; Li, Y. J.; Han, L.; Gao, J. R.; Wang, X. *Appl. Clay Sci.* **2011**, *51*, 360.
18. Wang, J. B.; Wang, G. J. *Surf. Coat. Technol.* **2011**, *11*, 37.
19. Becker, C. M.; Gabbardo, A. D.; Wypych, F.; Amico, S. C. *Compos. A* **2011**, *42*, 196.
20. Huang, J. B.; Chen, S. Q.; Song, P. G.; Lu, P. P.; Wu, C. G.; Liang, H. D. *Appl. Clay Sci.* **2014**, *88*, 78.
21. Li, Y. F.; Zhang, B.; Pan, X. P. *Compos. Sci. Technol.* **2008**, *68*, 1954.
22. Deng, Y. J.; White, G. N.; Dixon, J. B. *J. Colloid. Interface Sci.* **2002**, *250*, 379.
23. Patakfalvi, R.; Dékány, I. *Appl. Clay Sci.* **2004**, *25*, 149.
24. Chang, Z. H.; Guo, F.; Chen, J. F.; Yu, J. H.; Wang, G. Q. *Prog. Polym. Sci.* **2007**, *92*, 1204.
25. Pavlidou, S.; Papaspyrides, C. D. *Prog. Polym. Sci.* **2008**, *33*, 1119.
26. Lecouvet, B.; Sclavons, M.; Bailly, C.; Bourbigot, S. *Polym. Degrad. Stab.* **2013**, *98*, 2268.
27. Dasari, A.; Yu, Z. Z.; Cai, G. P.; Mai, Y. W. *Prog. Polym. Sci.* **2013**, *38*, 1357.
28. Zhao, S. P.; Gao, H.; Ren, X. M.; Yuan, G. J.; Lu, Y. N. *J. Mater. Chem.* **2012**, *22*, 447.
29. Hou, G. X.; Chen, X. G.; Liu, J. J.; Sang, X. M. *Polym. Plast. Technol. Eng.* **2011**, *50*, 1208.
30. Zhu, S. P.; Chen, J. Y.; Zuo, Y.; Li, H. L.; Cao, Y. *Appl. Clay Sci.* **2011**, *52*, 171.
31. Yuan, B. H.; Bao, C. L.; Song, L.; Hong, N. N.; Liew, K. M.; Hu, Y. *Chem. Eng. J.* **2014**, *237*, 411.
32. Liu, X. S.; Gu, X. Y.; Zhang, S.; Jiang, Y.; Sun, J.; Dong, M. Z. *J. Appl. Polym. Sci.* **2013**, *130*, 3645.
33. Ma, H. Y.; Tong, L. F.; Xu, Z. G.; Fang, Z. P. *Appl. Clay Sci.* **2008**, *42*, 238.
34. Pärpärta, E.; Darie, R. N.; Popescu, C. M.; Uddin, M. A.; Vasile, C. *Mater. Des.* **2014**, *56*, 763.
35. Zhang, X. R.; Xu, Z. *Mater. Lett.* **2007**, *61*, 1478.
36. Sun, D. W.; Li, Y. F.; Zhang, B.; Pan, X. B. *Compos. Sci. Technol.* **2010**, *70*, 981.